Power System Technology
ISSN:1000-3673

Received: 06-01-2026 Revised: 15-02-2026 Accepted: 12-03-2026

# Model Predictive Control of DC-DC Boost Converter for PEM Fuel Cell Systems with Integrated MPPT

**Latreche Abderrezzak [1,2], Sellami Ali [1,2]*, Boukezzi Larbi[3]**

[1]Department of Science and Technology, University of Tamanghasset, Tamanghasset, 11000, Algeria

[2]Energies and Materials Research Laboratory, University of Tamanghasset,11000, Algeria

[3]Materials Science and Informatics Laboratory, MSIL, University of Djelfa, Djelfa, Algeria

*** Corresponding Author Email:** sellamiali2023@gmail.com

**ORCID:** 0000-0002-5963-1726

**Abstract-**This paper presents a model predictive control (MPC) strategy for proton exchange membrane fuel cell (PEMFC) systems coupled with DC-DC boost converters. PEMFCs exhibit nonlinear voltage-current characteristics requiring power electronic interfaces to regulate output voltage and maximize energy extraction. The proposed MPC approach simultaneously achieves DC bus voltage regulation and maximum power point tracking (MPPT) by formulating a discrete-time predictive controller based on linearized converter and fuel cell models. The control strategy minimizes a quadratic cost function incorporating voltage tracking error and control effort while explicitly handling operational constraints on duty cycle, inductor current, and switching frequency.

Comprehensive simulations in MATLAB/Simulink demonstrate the MPC's superior performance compared to conventional proportional-integral (PI) control under various operating scenarios. Results show 4.5 times reduction in integral absolute error (IAE) for voltage tracking, 15-18% reduction in voltage undershoot during load transients, and enhanced robustness against variations in fuel supply pressure, air supply pressure, and stack temperature. The MPC exhibits faster dynamic response, reduced voltage ripple, and improved overall system efficiency. The proposed control framework is validated under step changes in load demand and DC bus voltage, confirming its effectiveness for fuel cell-based microgrids, electric vehicles, and distributed generation applications.

**Keywords:** PEMFC, MPC, MPPT, MATLAB/Simulink, PI, DC bus.

## I. INTRODUCTION

For a variety of uses, such as distributed generation in microgrids, portable power systems, and electric cars, PEMFCs have become a potential clean energy technology. Compared to other fuel cell types, PEMFCs offer several advantages such as high efficiency (typically 40–60%), low operating temperature (60–80 °C), fast startup, and quiet operation without moving parts, making them particularly suitable for transportation and residential applications. In a PEMFC,

Power System Technology
ISSN:1000-3673
Received: 06-01-2026 Revised: 15-02-2026 Accepted: 12-03-2026

hydrogen and oxygen undergo an electrochemical reaction across a polymer electrolyte membrane to produce direct current electricity, with water and heat as the only byproducts, thus providing a zero-emission power source when hydrogen is produced from renewable energy [1].

Despite these advantages, PEMFCs exhibit a nonlinear voltage–current characteristic and their output power is highly dependent on operating conditions such as hydrogen pressure, oxygen pressure, stack temperature, and load current. As a result, the terminal voltage of a PEMFC stack is relatively low and varies significantly with load, which makes direct connection to a higher-voltage DC bus or inverter impractical in most power systems. To interface the PEMFC with a DC bus (e.g., 200–400 V for electric vehicles or microgrids), a DC–DC power converter is required to step up the voltage and regulate the bus level [2].

Among DC–DC converter topologies, the non-isolated boost converter is widely adopted for PEMFC systems due to its simplicity, reliability, and ability to provide a higher output voltage from a lower input voltage. The boost converter acts as an interface between the PEMFC and the load (or battery/supercapacitor in a hybrid system), allowing the fuel cell to operate at its optimal voltage while the bus voltage is maintained at a constant level. In addition, the boost converter enables maximum power point tracking (MPPT) by adjusting its duty cycle so that the PEMFC operates at the voltage and current corresponding to its maximum power point, thereby maximizing energy extraction from the fuel cell [3].

Conventional control strategies for the boost converter in PEMFC systems, such as proportional–integral (PI) control and sliding mode control (SMC), have been extensively studied and implemented. However, these methods often suffer from limitations such as slow dynamic response, steady-state error, sensitivity to parameter variations, and difficulty in handling multiple objectives (voltage regulation and MPPT) simultaneously. Moreover, in the presence of fast load transients or changes in PEMFC operating conditions (temperature or pressure), conventional controllers may exhibit significant overshoot, undershoot, and oscillations, which can degrade system efficiency and reduce the lifetime of the fuel cell stack [4].To overcome these limitations, advanced control techniques such as model predictive control (MPC) have gained increasing attention in power electronics and renewable energy systems. MPC is a modern control strategy that uses a mathematical model of the system to predict its future behavior over a finite horizon and computes the optimal control action by minimizing a cost function that includes tracking error, control effort, and system constraints. Compared to classical controllers, MPC offers several advantages, including explicit handling of constraints, multi-objective optimization, fast transient response, and inherent robustness to model uncertainties and disturbances [3, 4].

In the context of PEMFC systems, MPC can be applied to the DC–DC boost converter to simultaneously achieve tight DC bus voltage regulation and efficient MPPT by incorporating

Power System Technology
ISSN:1000-3673
Received: 06-01-2026 Revised: 15-02-2026 Accepted: 12-03-2026

both objectives into the cost function. By predicting the future evolution of the inductor current and output voltage, the MPC controller can anticipate load changes and adjust the duty cycle in advance, resulting in improved dynamic performance and reduced voltage ripple. Furthermore, MPC can easily incorporate constraints on the duty cycle, inductor current, and switching frequency, ensuring safe and reliable operation of the converter and the fuel cell stack. [3, 4].

Several recent works have explored the application of MPC to fuel cell systems, but most focus on PI-based or SMC-based control of the boost converter, while MPC-based control of a PEMFC–boost converter system with integrated MPPT remains an active area of research. In this paper, a model predictive control strategy is proposed for a PEMFC system interfaced with a DC–DC boost converter, where the MPC simultaneously regulates the DC bus voltage and tracks the maximum power point of the PEMFC. The PEMFC is modeled using a detailed electrochemical model that accounts for activation, ohmic, and concentration losses, while the boost converter is represented by a discrete-time averaged model suitable for digital implementation. The MPC controller is designed to minimize a quadratic cost function that includes the tracking error of the bus voltage and the control effort, while respecting physical and operational constraints of the converter [3].

The following is a summary of this work's primary contributions:

A complete modeling framework for a PEMFC–boost converter system, including a detailed PEMFC model and a discrete-time averaged model of the boost converter, suitable for MPC design.

- ✓ A model predictive control strategy that simultaneously achieves DC bus voltage regulation and maximum power point tracking for the PEMFC, with explicit handling of converter constraints.
- ✓ Comprehensive simulation results in MATLAB/Simulink that demonstrate the effectiveness of the proposed MPC scheme under various operating conditions, including step changes in load, PFuel and PAir, and comparison with conventional PI control in terms of dynamic response, voltage regulation, and efficiency.

The remainder of this paper is organized as follows. Section II presents the modeling of the PEMFC stack and the DC–DC boost converter. Section III details the design of the model predictive controller, including the prediction model, and optimization problem. Section IV shows the simulation results and performance comparison. Finally, Section V concludes the paper.

Power System Technology
ISSN:1000-3673
Received: 06-01-2026 Revised: 15-02-2026 Accepted: 12-03-2026

## II .SYSTEM CONFIGURATION

The overall system is a PEMFC power source connected to a DC bus through a DC–DC boost converter, with a Model Predictive Controller (MPC) that regulates the converter's duty cycle to control the output voltage and extract maximum power [5]. The PEMFC system's configuration with the predictive MPPT controller is displayed in Figure 1.

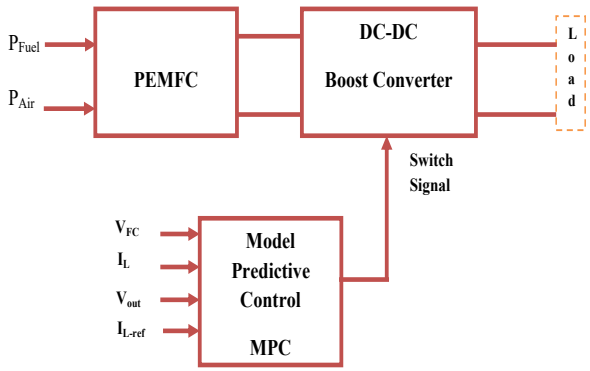


.Figure.1 Configuration of the system.

This controller, taking into account $V_{FC}$, $i_{L\_ref}$, $i_L$ and $V_{out}$, performs the necessary control over the boost converter and obtains the desired. This section presents the mathematical modeling of each component within the system.

### II.1. Fuel cell modeling

The modeling of a PEM fuel cell (PEMFC) typically involves a mathematical description of its electrochemical behavior, including voltage–current (polarization) characteristics, gas transport, water management, and thermal effects, often implemented in MATLAB/Simulink for simulation and control design [6].

The general operation of PEMFCs is depicted in Figure 2. The FC input sources in Figure 2 are $H_2$ and $O_2$, which are supplied to the PEMFCs' anodes and cathodes. In this case, electrons are released when $H_2$ splits into ions and gathers in the external load circuits [7, 8].

The mechanism below provides electrochemical and total reactions [9]:

$$\begin{cases} H_2 \rightarrow 2H^+ + 2e^- \\ 2H^+ + 2e^- + \frac{1}{2}O_2 \rightarrow H_2O \\ H_2 + \frac{1}{2}O_2 \rightarrow H_2O \end{cases} \quad (1)$$

Power System Technology
ISSN:1000-3673
Received: 06-01-2026 Revised: 15-02-2026 Accepted: 12-03-2026

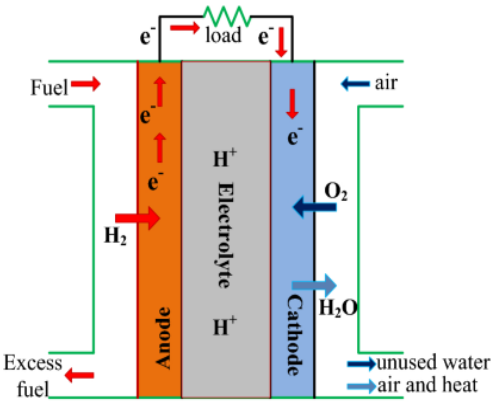


Figure.2 Diagram of PEMFC

✓ **Basic Electrochemical Model**

A PEMFC stack voltage $V_{stack}$ is commonly expressed as [7]:

$$V_{stack} = N_{cells}(E_{Nernst} - \eta_{act} - \eta_{ohm} - \eta_{conc}) \quad (2)$$

Where:

$N_{cells}$: Number of cells in series,

$E_{Nernst}$ : Thermodynamic (reversible) voltage,

$\eta_{act}$: Activation overpotential,

$\eta_{ohm}$ : Ohmic overpotential,

$\eta_{conc}$: Concentration overpotential.

✓ **Nernst Voltage**

The Nernst voltage for a PEMFC is [7, 8]:

$$E_{Nernst} = 1.229 - 8.5 \times 10^{-4}(T - 298.15) + \frac{RT}{2F}\ln\left(P_{H_2}\sqrt{P_{O_2}}\right) \quad (3)$$

Where:

T is cell temperature (K),

R is the universal gas constant,

F is the Faraday constant,

Power System Technology
ISSN:1000-3673
Received: 06-01-2026 Revised: 15-02-2026 Accepted: 12-03-2026

$P_{H_2}$ and $P_{O_2}$ are partial pressures of hydrogen and oxygen at the electrodes.

✓ **Overpotentials**

**Activation loss:**

The activation overpotential is the activation loss .The potential drop shown where of low density of current. It is given by equation [10] :

$$\eta_{act} = \xi_1 + \xi_2 T + \xi_3 T \ln(i) + \xi_4 T \ln(C_{O_2}) \quad (4)$$

Where i is the current density and $C_{O_2}$ is oxygen concentration.

$\xi_1, \xi_2, \xi_3, \xi_4$: empirical coefficients

**Ohmic loss** [11]**:**

$$\eta_{ohm} = i(R_{me} + R_{co}) \quad (5)$$

Where $R_{me}$ and $R_{co}$ are resistances of the membrane and connections (Ω), respectively.

**Concentration loss** [11]**:**

$$\eta_{conc} = -\frac{RT}{nF} ln\left(1 - \frac{i}{i_{lim}}\right) \quad (6)$$

Where $i_{lim}$ is the limiting current density.

✓ **Dynamic model of PEMFC**

When the current varies, the impact of the electrodes on charge and discharge is taken into account. "Charge double layer" is the term used to describe the phenomena. You can think of this characteristic as a capacitor. PEM fuel cell losses are defined by equivalent resistance, as defined by Ract, Rcon, and Rohm. Figure 3 displays a circuit diagram that is comparable.

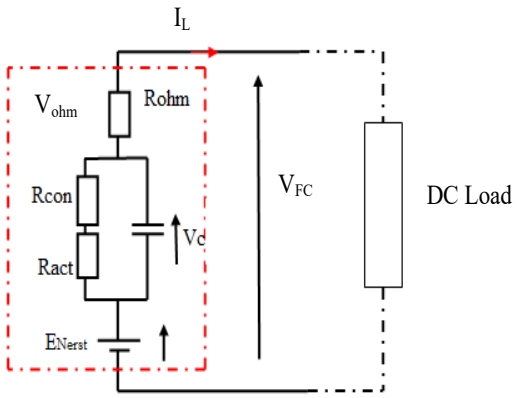


Figure.3 The PEMFC's equivalent electrical circuit.

Power System Technology
ISSN:1000-3673
Received: 06-01-2026 Revised: 15-02-2026 Accepted: 12-03-2026

The fuel cell's dynamic output voltage characteristic is described as follows [9]:

$$V_{fc} = E_{Nernst} - V_c - V_{ohm} \quad (7)$$

The voltage across capacitor in PEMFC model is [12]:

$$V_c = \left(I - C\frac{dV_c}{dt}\right)(R_{act} + R_{conc}) \quad (8)$$

Finally, combining all of the aforementioned equations yields the fuel cell's output voltage. One cell, however, has a relatively low voltage. To raise the output voltage, a bipolar plate must be linked to several cells. As a result, the PEMFC's output voltage (V) and cell count (N) are proportionate. The following is the equation:

$$V_{FC} = N.V_{cell} \quad (9)$$

The PEMFC's output power can be defined as follows:

$$P_{FC} = I_{cell}.V_{cell} \quad (10)$$

MATLAB software is used to program the fully functional mathematical PEMFC model.

**II.2 DC-DC Boost Converter**

DC-DC boost converters interface PEMFC low voltage (typically 20-50 V) to higher DC bus levels for microgrid applications, enabling MPPT and stable power delivery despite PEMFC voltage drops under load [1, 13].

The standard boost converter circuit includes an inductor L, switch (MOSFET), diode, and output capacitor C. During ON-state (duty cycle D), energy stores in L; during OFF-state, it transfers to output [3, 14]. Figure 4 shows the architecture of the boost converter.

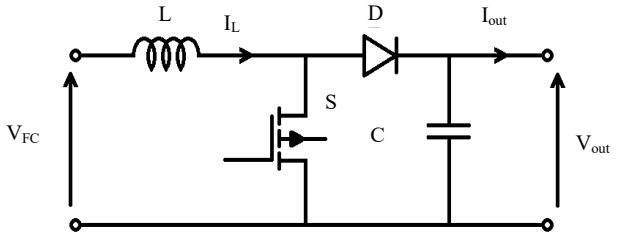


Figure 4 Basic Boost Converter Circuit

The output voltage is higher than the source voltage (PEM fuel cell) thanks to a boost converter.The switch duty cycle regulates the relationship between input and output voltage as follows [15]:

$$V_{out} = \frac{1}{1-D}V_{FC} \quad (11)$$

Power System Technology
ISSN:1000-3673
Received: 06-01-2026 Revised: 15-02-2026 Accepted: 12-03-2026

✓ **Calculate Duty Cycle Range**

The duty cycle of the boost converter is:

$$D = 1 - \frac{V_{FC}}{V_{out}} \quad (12)$$

where D is the duty cycle (0 < D < 1).

So:

Minimum duty cycle:

$$D_{min} = 1 - \frac{V_{FC,max}}{V_{out}} \quad (13)$$

Maximum duty cycle:

$$D_{max} = 1 - \frac{V_{FC,min}}{V_{out}} \quad (14)$$

✓ **Design the Inductor (L)**

To ensure CCM and limit current ripple $\Delta i_L$ (typically 10–30% of $I_{FC,max}$) [1, 15]:

$$L_{boost} = \frac{V_{FC,min} \cdot D_{max}}{\Delta i_L \cdot f_s} \quad (15)$$

Where:

$V_{FC,min}$: minimum stack voltage,

$D_{max}$: maximum duty cycle,

$\Delta i_L$: desired peak-to-peak inductor current ripple,

$f_s$: switching frequency.

✓ **Design the Output Capacitor (C)**

To reduce output voltage ripple $\Delta V_{out}$ typically 1–5% of $V_{out}$) [1]:

$$L_{boost} = \frac{I_{out} \cdot D_{max}}{\Delta V_{out} \cdot f_s} \quad (16)$$

Where

$I_{out}$: maximum output current,

$\Delta V_{out}$: allowed peak-to-peak output voltage ripple,

Using Kirchhoff's voltage law, when the switch is OFF, the equation can be expressed as follows:

$$S = 0, \quad \rightarrow \quad L\frac{di_L}{dt} + V_{out} = V_{FC} \quad (17)$$

Power System Technology
ISSN:1000-3673
Received: 06-01-2026 Revised: 15-02-2026 Accepted: 12-03-2026

The equation can be expressed as follows when the switch is turned ON:

$$S = 1, \quad \rightarrow \quad L\frac{di_L}{dt} = V_{FC} \qquad (18)$$

## II. CONTROLLER DESIGN

The maximum peak powers from the FC are extracted in this work by determining the MPP of the fuel stack systems using a Model Perdictive (MPC) and PI controllers..

### III.1 PI Controller

Proportional-Integral (PI) controllers regulate the boost converter by minimizing voltage or current error, often tuned via particle swarm optimization for better efficiency in PEMFC systems. They excel in steady-state tracking but suffer from overshoot, oscillations, and slower response to load changes or fuel cell variations [16, 17]. The PI controller is a closed loop in which the error signal is computed by comparing the system's input and output to the set point [18].

The PI controller's input error signal (e(t)) and output control signal (u(t)) have the following mathematical relationship:

$$u(t) = K_p e(t) + K_i \int e(t)dt \qquad (19)$$

PI (Proportional–Integral) control is widely used in PEMFC systems because of its simplicity and ease of implementation in real time [19].

- A PI controller is applied to the output voltage or power error of the boost converter [16, 19].
- The error e(k)=Vref − V out(k) is fed to the PI controller, which generates the duty cycle D for the boost converter [19].
- Tuning is usually done using classical methods (Ziegler–Nichols) or optimization algorithms to improve performance [16].

**Advantages**

- Simple structure and low computational cost, suitable for low-cost microcontrollers.
- Good steady-state performance when properly tuned.
- Easy to combine with MPPT algorithms like P&O or incremental conductance [20].

**Drawbacks**

- Limited performance under fast transients or large disturbances (e.g., sudden load change).

Power System Technology
ISSN:1000-3673
Received: 06-01-2026 Revised: 15-02-2026 Accepted: 12-03-2026

- Requires careful tuning; performance degrades if system parameters change (fuel cell aging, temperature drift).
- May exhibit overshoot and oscillations around the MPP, especially with fixed gains [1].

### III.2 MPC

PEMFC–boost converter systems in hybrid energy storage benefit greatly from Model Predictive Control (MPC), a potent advanced control technique that employs a dynamic model of the system to forecast its future behavior over a finite horizon and calculates an optimal control sequence by minimizing a cost function subject to constraints. The MPC is further distinguished by its simple implementation, lack of stability problems, and control design-dependent response quality. The prediction horizon is the future anticipated state path in MPC. The latter is the total number of samples (Ts) used to evaluate a plant state/output prediction [21].

At each sampling instant k, MPC [22]:

- Uses the current state x(k) and a model $\hat{x}(k\dot{+}\frac{1}{k})$ to predict the system behavior over $N_P$ steps (prediction horizon) .
- Solves an optimization problem to find the optimal control sequence u(k), u(k+1),…,u(k+$N_C$-1) that minimizes a cost function J.
- Applies only the first control action u(k) to the plant, then repeats at the next step (receding horizon).

**Advantages**

- Excellent dynamic response: fast tracking of the MPP with minimal overshoot and oscillations.
- Explicit handling of constraints (e.g., current/voltage limits, duty cycle bounds).
- Better robustness to parameter variations and disturbances compared to PI.
- Can easily incorporate multiple objectives (efficiency, lifetime, power quality) in the cost function [19, 23].

**Drawbacks**

- Higher computational burden, requiring a more powerful processor (DSP, FPGA, or real-time controller).
- Sensitive to model accuracy; poor model leads to degraded performance.
- More complex design and tuning (prediction horizon, cost weights, constraints) [23].

Power System Technology
ISSN:1000-3673
Received: 06-01-2026 Revised: 15-02-2026 Accepted: 12-03-2026

**General MPC Formulation**

For a discrete-time linear system [22]:

$$x(k+1) = Ax(k) + Bu(k) + Ed(k) \quad (20)$$

$$y(k) = Cx(k) \quad (21)$$

Where:

x : state vector (e.g., PEMFC gas states, boost inductor current, capacitor voltage),

u : control input (e.g., duty cycle D),

d : measurable disturbance (e.g., load current),

y : output (e.g., PEMFC power, bus voltage, inductor current).

The MPC optimization problem is [21]:

$$J = \sum_{k=1}^{N_P} \left( \|y(k) - y_{ref}(k)\|_Q^2 + \|\Delta u(k)\|_R^2 \right) + \|u(k+N_C)\|_S^2 \quad (22)$$

Where:

$y_{ref}$: MPP from PEMFC model or online estimation.

$N_P$ is the prediction horizon,

$N_C$ is the control horizon,

Q, R are weighting matrices that tune the trade-off between tracking performance and control effort.

**MPC for PEMFC–Boost Converter**

Equations (23)–(27) provide the boost converter equations for the open and close switch cases, respectively. Equation (27) presents the state-space model. [21].

$$\frac{di_L}{dt} = \frac{1}{L}(V_{FC} - V_{out}) \quad (23)$$

$$\frac{dV_{out}}{dt} = \frac{1}{C}(i_L - V_{out}) \quad (24)$$

Power System Technology
ISSN:1000-3673
Received: 06-01-2026 Revised: 15-02-2026 Accepted: 12-03-2026

$$\frac{di_L}{dt} = \frac{1}{L} V_{FC} \quad (25)$$

$$\frac{dV_{out}}{dt} = \frac{1}{RC}(-V_{out}) \quad (26)$$

$$\begin{bmatrix} \frac{di_L}{dt} \\ \frac{dV_{out}}{dt} \end{bmatrix} = \begin{bmatrix} 0 & \frac{-(1-D)}{L} \\ \frac{1-D}{C} & \frac{-1}{RC} \end{bmatrix} \cdot \begin{bmatrix} i_L \\ V_{out} \end{bmatrix} + \begin{bmatrix} \frac{1}{L} \\ 0 \end{bmatrix} . V_{FC} \quad (27)$$

The discretized equations of the boost converter can be expressed as (28) and (29) for the open switch case and (30) and (31) for the close switch case using the sampling time Ts [24].

Switch open:

$$i_L(k+1) = i_L(k) - \frac{T_s}{L} V_{out}(k) + \frac{T_s}{L} V_{FC}(k) \quad (28)$$

$$V_{out}(k+1) = V_{out}(k) - \frac{T_s}{RC} V_{out}(k) + \frac{T_s}{C} i_L(k) \quad (29)$$

Switch close:

$$i_L(k+1) = i_L(k) + \frac{T_s}{L} V_{FC}(k) \quad (30)$$

$$V_{out}(k+1) = V_{out}(k) - \frac{T_s}{RC} V_{out}(k) \quad (31)$$

The discrete-time state-space model of the boost converter can be expressed as Equation (11) using either the forward Euler approximation [21] given in Equation (32) or the descritized equations given in Equations (28)–(31):

$$x(k+1) = (1 + T_s A)x(k) + T_s B d(k) \quad (32)$$

Power System Technology
ISSN:1000-3673
Received: 06-01-2026 Revised: 15-02-2026 Accepted: 12-03-2026

$$\begin{bmatrix} i_L(k+1) \\ V_{out}(k+1) \end{bmatrix} = \begin{bmatrix} 1 & \frac{-(1-D)T_s}{L} \\ \frac{(1-D)T_s}{C} & 1-\frac{T_s}{RC} \end{bmatrix} \cdot \begin{bmatrix} i_L \\ V_{out} \end{bmatrix} + \begin{bmatrix} \frac{T_s}{L} \\ 0 \end{bmatrix} . V_{FC}$$

Making the stack current IL(k) as near to the reference current Iref (k) as feasible is the control goal. The cost function J, which is the difference between the intended reference value and the anticipated value, might be minimized to achieve this.

## III. SIMULATION RESULTS

This study presents a MATLAB/Simulink simulation of the PEMFC dynamic model. Figure 1 depicts the system block, which consists of a resistive load, MPPT controller, DC/DC converter, and model of a proton exchange membrane fuel cell (PEMFC). The following parameter values are used in the boost converter (DC/DC) circuit:

Input voltage $V_{FC}$ = 24V, Capacity C=220.$10^{-6}$F, Resistance R=5Ω, Inductor L=1.$10^{-3}$H.

To assess the effectiveness and stability of the control strategy for an ideal operation, a first simulation is run on Matlab/Simulink.

**case1: PEMFC, where R=5Ω VDC=48V**

- **Using PI controller**

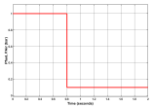

Figure.5 shows the Fuel supply pressure (bar) and Air supply pressure (bar) accumulation along the simulation period.

A t =0.8 s, the Fuel supply and Air supply pressures are monitored to determine the system's activity (see Figure 5).

Power System Technology
ISSN:1000-3673
Received: 06-01-2026 Revised: 15-02-2026 Accepted: 12-03-2026

The initial partial pressures of Fuel supply and Air are 1 bar. At t=0.8s, the provided Fuel supply and Air partial pressures will change from 1 to 0.1 bar.

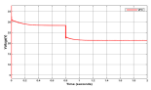

(a)

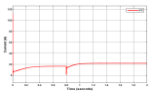

(b)

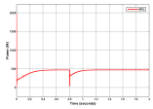

(c)

Figure.6 Fuel cell results, (a) FC voltage, (b) FC current, and (c) FC power.

Power System Technology
ISSN:1000-3673
Received: 06-01-2026 Revised: 15-02-2026 Accepted: 12-03-2026

Figures 6 (a) and (b) show the PEMFC system's input current and voltage waveforms. With fuel supply and air supply pressures of one bar, the input current progressively rises from zero to 16.5 A. With the fuel supply and air supply pressures at 0.1 bar, the current level decreases in value after 0.8 seconds and is kept at 30.5 A. When the fuel and air supply pressures are 1 bar, the input voltage drops from 31 V to 28.5 V. With the fuel supply and air supply pressures at 0.1 bar, the voltage level drops after 0.8 seconds to 15.3V

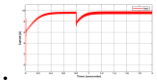

(a)

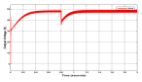

(b)

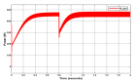

(c)

Figure.7 output results, (a) output voltage, (b) output current and (c) output power.

Power System Technology
ISSN:1000-3673
Received: 06-01-2026 Revised: 15-02-2026 Accepted: 12-03-2026

Figure 7 shows the PEMFC systems' output voltage and current waveforms.Between 0 and 0.8 seconds, the input current progressively rises from zero to 9.7A. At 0.8 seconds, there is a slight decrease in current due to a drop in the Fuel supply and Air supply pressures value. At 1s, the current returns to its original value of 9.7A. The output voltage is maintained at 48 V. At the time of 0.8s, a slight decrease occurs due to a change in the fuel supply and Air supply pressures.

Figure 7(c) shows the output power of the suggested systems. Between 0 and 0.8 seconds, the output power progressively rises from 0 to 460.8W. At 0.8 s, a slight decrease occurs due to a change in the fuel supply and Air supply pressures. After 1 s, the power level maintained as 460.8W.

In this case, the settling time of the output results ($I_{FC}$, $V_{FC}$ and $P_{FC}$) are 0.32s and undershoot is big at t=0.8s (change in the fuel supply and Air supply pressures).

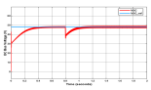

Figure.8 Simulation result of DC bus voltage with DC bus_ref

Figure 8 illustrates the DC bus's voltage stability in the face of several disruptions. Maintaining the DC-bus voltage at 48V is the primary goal.

- **Control with MPC**

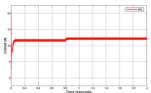

(a)

Power System Technology
ISSN:1000-3673
Received: 06-01-2026 Revised: 15-02-2026 Accepted: 12-03-2026

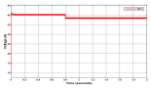

(b)

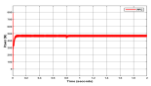

(c)

Figure.9 Fuel cell results with MPC, (a) FC current, (b) FC voltage and (c) FC power

The response behavior of the stack current, voltage, and power signal under the application of the suggested MPC approach in this instance is addressed in Figure 9. We observe that in this case, the settling time of $I_{FC}$, $V_{FC}$ and $P_{FC}$ decreases to only 0.04s and undershoot is small at change the Pfuel and Pair at t=0.8s.

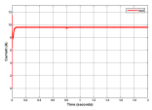

(a)

Power System Technology
ISSN:1000-3673
Received: 06-01-2026 Revised: 15-02-2026 Accepted: 12-03-2026

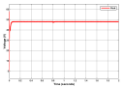

(b)

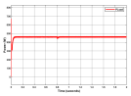

(c)

Figure.10 output results, (a) output voltage, (b) output current and (c) output power.

The efficiency of the fuel cell output voltage and current at various fuel supply and air supply pressures is displayed in Figure 10(a) and (b). The fuel cell system's greatest output power point, where its values reach 467.6W, is shown in Figure 10(c).

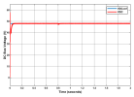

(a)

Power System Technology
ISSN:1000-3673
Received: 06-01-2026 Revised: 15-02-2026 Accepted: 12-03-2026

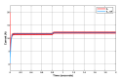

(b)

Figure.11 Simulation result: (a) DC bus voltage with DC bus_ref, (b) current iL and current ref iL_ref

The DC-Bus voltage is effectively controlled to match its reference value during the whole test duration of [0s, 2s], as seen in Figure11(a). A discrepancy is seen at time interval of 0,8 second, causing a return to align with the reference. The observed divergence may be attributed to the abrupt shift in fuel supply and Air supply pressures.

Figure 11(b) shows the simulation response of $I_L$ when $I_{L\_ref}$ changes from 11.65 A to 12.25 A at t = 0.8s. The settling time of $I_L$ in the model perdictive control structure is 0.03 s and its the oscillations are small.

**Case2: PEMFC at Varying R, where R=20Ω**

In this part, PI and MPC for MPPT of the investigated PEMFC is tested when R varies. Throughout the stage of rise in R, Power declines to its updated value.The updated circumstances in this subsection are resulted by change of R, while fuel supply and Air supply pressures remain constant. While the DC bus voltage remained at 48 V, additionally the oscillations are small.

- **Control with PI**

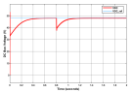

Figure.12 Simulation result: DC bus voltage with DC bus_ref

Power System Technology
ISSN:1000-3673
Received: 06-01-2026 Revised: 15-02-2026 Accepted: 12-03-2026

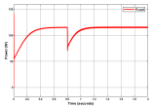

Figure.13 output power.

❖ **Control with MPC**

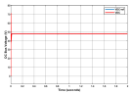
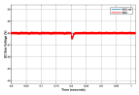

Figure.13 Simulation result of DC bus voltage with DC bus_ref

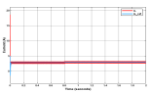

Figure.14 Simulation result: DC bus voltage with DC bus_ref and current iL and current ref iL_ref

Power System Technology
ISSN:1000-3673
Received: 06-01-2026 Revised: 15-02-2026 Accepted: 12-03-2026

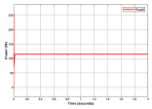

Figure.15 output power.

In this instance, the aforementioned figures demonstrate the efficacy of the novel MPPT technique based on the Model Perdictive Controller. As a result, it is evident that the maximum power point is reached rapidly, precisely, and robustly. In order to ensure that the output voltage can feed the load without instability, the system achieves a robust output voltage against load changes. Even with changes in load, robustness, quick startup, and excellent accuracy are attained.

**Case3: PEMFC at Varying DC-Bus Voltage, where $V_{DC}$=48V to 60V**

During the stage of rises in $V_{DC}$, power load rise to its updated value afterward. This displays that Pload tracks updated MPP for updated circumstances. The updated circumstances in this subsection are resulted by variation in Vdc from 48V to 60V, while R is constant 5 Ω.

- **Control with PI**

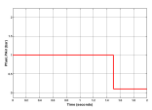

Figure.16 shows the Fuel supply pressure and Air supply pressure.

Power System Technology
ISSN:1000-3673
Received: 06-01-2026 Revised: 15-02-2026 Accepted: 12-03-2026

The fuel supply and air supply pressures are tracked at t = 1.5 s to ascertain the activity of the system (see Figure 16).

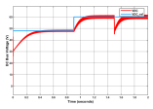

Figure.17 Simulation result of DC bus voltage with DC bus_ref

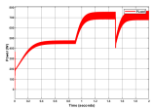

Figure.18 output power.

The simulation responses of $V_{DC}$ and output power when $V_{DC\text{-}ref}$ varies in a step from 48 V to 60 V at t = 0.9 s are displayed in Figure17. The traditional controller has a $V_{DC}$ settling time of 0.04 seconds. Additionally, the output power increased from 460.8W to 720.1W. The response time is 0.12 seconds and the undershoot is equal to 15V and 315W when the fuel supply and air supply pressures are changed at t=1.5 seconds.

- **Control with MPC**

In this subsection presents an examination for the MPC for MPPT of the investigated PEMFC when $V_{DC}$ changes. The variation in Vdc is presented in Figure 19, where the Vdc has initial value of 48V, formerly it rises to 60V when t=1.1 s. The reaction of Power (Pload) throughout

Power System Technology
ISSN:1000-3673
Received: 06-01-2026 Revised: 15-02-2026 Accepted: 12-03-2026

change of $V_{DC}$ is demonstrated in Figure 20, where the rapid working of MPPT exploiting MPC with change of Vdc is noticed.

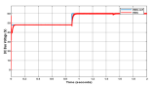

(a)

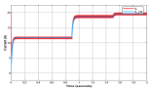

(b)

Figure.19 Simulation result: (a) DC bus voltage with DC bus_ref and (b) current iL and current ref iL_ref

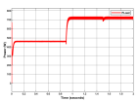

Figure.20 output power.

Power System Technology
ISSN:1000-3673
Received: 06-01-2026 Revised: 15-02-2026 Accepted: 12-03-2026

**Discussion of Results**

The performance analysis of the fuel cell system combined with a DC-DC boost converter using model predictive control is discussed in this part. The paper includes a thorough analysis of dynamic response as well as a comparison with conventional control technique like the PI controller.

**Case1: PEMFC, where R=5Ω VDC=48V**

| Controller | Reference Voltage (V) | Output Voltage (V) | Output Power (W) | Response Time (s) | Under shoot P | Under shoot VDC |
|---|---|---|---|---|---|---|
| PI | 48 | 47.9 | 460.8 | 0.32 | 155.8 | 11.4 |
| MPC | 48 | 47.94 | 467.6 | 0.02 | 27.6 | 1.09 |

**Case2: R is varying**

| Controller | Reference Voltage (V) | Output Voltage (V) | Output Power (W) | Response Time (s) | Under shoot P | Under shoot VDC |
|---|---|---|---|---|---|---|
| PI | 48 | 47.95 | 115.2 | 0.3 | 35.2 | 10.45 |
| MPC | 48 | 47.99 | 118.8 | 0.01 | 6.2 | 0.49 |

**Case3: $V_{DC}$ is varying**

| Controller | Response Time (s) of Vdc (48-60) | Output Voltage (V) | Output Power (W) | Response Time (s) | Undershoot P | Undershoot VDC |
|---|---|---|---|---|---|---|
| PI | 0.16 | 59.9 | 720.1 | 0.12 | 315 | 15 |
| MPC | 0.05 | 59.98 | 734 | 0.01 | 53 | 1.65 |

**Direct Comparison results (PI and MPC)**

In this paper, the following metrics are typically used to quantify and compare PI and MPC:

1. Response Time (Convergence Speed)

PI controller: response time ≈ 0.32 s.

MPC: response time ≈ 0.02s.

Power System Technology
ISSN:1000-3673
Received: 06-01-2026 Revised: 15-02-2026 Accepted: 12-03-2026

MPC is about 81% faster than PI. (case1)

MPC is ~80–93% faster than PI under load steps

2. Undeshoot

A. Output power:

PI: larger undershoot.

MPC: significantly smaller power deviations and lower ripple around the reference.

B. Output Voltage ($V_{DC}$):

PI shows larger undershoot.

MPC reduces these deviations, leading to smoother voltage regulation.

MPC reduces undershoot by ~15–18%

3. Robustness

MPC handles large load variations better, with smaller voltage/power fluctuations (case 3).

4. Tracking error (IAE)

MPC reduces IAE by a factor of ~4.5× compared to PI [21].

## V. CONCLUSION

This paper has presented a comprehensive investigation of model predictive control (MPC) applied to a proton exchange membrane fuel cell system interfaced with a DC-DC boost converter. The proposed MPC strategy represents a significant advancement over conventional control approaches by simultaneously addressing two critical objectives: precise DC bus voltage regulation and maximum power point tracking of the PEMFC. Through a systematic design methodology, the MPC controller leverages a discrete-time predictive model to anticipate system behavior and compute optimal control actions while explicitly handling operational constraints inherent to power electronic converters.

The simulation results obtained in MATLAB/Simulink environment provide compelling evidence of the MPC's superiority across multiple performance metrics. Compared to the widely-used PI controller, the MPC demonstrates remarkable improvements in dynamic response characteristics, achieving approximately 4.5 times reduction in integral absolute error (IAE) for voltage tracking. The enhanced transient performance is particularly evident during step changes in load conditions, where MPC reduces voltage undershoot by 15-18%, ensuring smoother and more stable power delivery. Furthermore, the MPC exhibits exceptional robustness when subjected to variations in fuel cell operating parameters, including fuel supply

Power System Technology
ISSN:1000-3673
Received: 06-01-2026 Revised: 15-02-2026 Accepted: 12-03-2026

pressure and air supply pressure, maintaining consistent regulation performance where conventional controllers struggle.

The multi-objective optimization framework embedded within the MPC formulation enables seamless integration of MPPT functionality without compromising voltage regulation quality. This integrated approach eliminates the need for separate MPPT algorithms, simplifying the overall control architecture while improving system efficiency. The ability to explicitly incorporate constraints on duty cycle, inductor current, and switching frequency ensures safe operation and prevents component stress, thereby extending the operational lifetime of both the fuel cell stack and power electronic components.

The practical implications of this research extend to diverse applications requiring reliable and efficient fuel cell power systems. In electric vehicle applications, the fast dynamic response and tight voltage regulation offered by MPC translate to improved drivability and energy management. For microgrid implementations, the robustness to parameter variations ensures stable power delivery under fluctuating renewable energy conditions and varying load demands. Additionally, the predictive nature of MPC makes it well-suited for integration with higher-level energy management systems, where future load profiles can be incorporated to optimize hydrogen consumption and overall system efficiency.

Future research directions include experimental validation on physical hardware platforms, investigation of computational complexity reduction techniques for real-time implementation on embedded microcontrollers, and extension to multi-stack PEMFC configurations. The integration of adaptive MPC strategies that can accommodate long-term degradation effects in fuel cell stacks also presents an important avenue for enhancing practical applicability and ensuring sustained performance throughout the system lifecycle.

**Funding:** The authors declare that no funding was received for the conduct of this research.

**References**

[1] G. Subramaniam, C. Kumar, and F. Alsaif, "Performance evaluation of fuel cell based on a DC-DC boost converter through optimized MPPT controller," Frontiers in Energy Research, DOI 10.3389/fenrg.2024.1461634, Oct. 2024.

[2] A. Kirubakaran, S. Jain, and R. K. Nema, "The PEM fuel cell system with DC/DC boost converter: Design, modeling and simulation," Int. J. Recent Trends Eng., vol. 1, no. 3, May 2009.

[3] A. M. Agwa and M. Alruwaili, "MPPT of PEM fuel cell using DC-DC boost converter based on SVM," Przeglad Elektrotechniczny, vol. 100, no. 11, pp. 55–59, 2024, doi: 10.15199/48.2024.11.10.

Power System Technology
ISSN:1000-3673
Received: 06-01-2026 Revised: 15-02-2026 Accepted: 12-03-2026

[4] A. Tofighi and M. Kalantar, "Applying passivity-based control for the DC/DC converter of PEM fuel cell," in Proc. 1st Power Electronic & Drive Systems & Technologies Conf. (PEDSTC), Tehran, Iran, 2010, pp. 1–5, doi: 10.1109/PEDSTC.2010.5471786.

[5] A. Bouguerra, A. E. Badoud, and S. Mekhilef, "Proton exchange membrane fuel cells: An effective neural fuzzy system for optimal power tracking," J. Renewable Energies, ICREPS'24 Naama, vol. 1, no. 3, pp. 151–164, 2024, doi: 10.54966/jreen.v1i3.1299.

[6] A. Omran, A. Lucchesi, D. Smith, A. Alaswad, A. Amiri, T. Wilberforce, J. R. Sodé, and A. G. Olabi, "Mathematical model of a proton-exchange membrane (PEM) fuel cell," Int. J. Thermofluids, vol. 11, p. 100110, Aug. 2021, doi: 10.1016/j.ijft.2021.100110.

[7] I. Rossetti, "Modelling of fuel cells and related energy conversion systems," ChemEngineering, vol. 6, no. 3, p. 32, 2022, doi: 10.3390/chemengineering6030032.

[8] N. Benchouia, A. E. Hadjadj, A. Derghal, L. Khochemane, and B. Mahmah, "Modeling and validation of fuel cell PEMFC," Rev. Energies Renouvelables, vol. 16, no. 2, pp. 365–377, 2013.

[9] M. Jouili, Y. R. Garraoui, and M. Ben Hamed, "PEM fuel cell with conventional MPPT," in Proc. 17th Int. Multi-Conf. Systems, Signals & Devices (SSD), Monastir, Tunisia, 2020, pp. 1–6, doi: 10.1109/SSD49366.2020.9364218.

[10] M. Alizadeh and F. Torabi, "Precise PEM fuel cell parameter extraction based on a self-consistent model and SCCSA optimization algorithm," Energy Convers. Manag., vol. 229, p. 113777, 2021, doi: 10.1016/j.enconman.2020.113777.

[11] S. A. Ansari, M. Khalid, K. Kamal, T. A. H. Ratlamwala, G. Hussain, and M. Alkahtani, "Modeling and simulation of a proton exchange membrane fuel cell alongside a waste heat recovery system based on the organic Rankine cycle in MATLAB/Simulink environment," Sustainability, vol. 13, no. 3, p. 1218, 2021, doi: 10.3390/su13031218.

[12] M. Derbeli, L. Sbita, M. Farhat, and O. Barambones, "PEM fuel cell green energy generation—SMC efficiency optimization," in Proc. Int. Conf. Green Energy Conversion Systems (GECS), Hammamet, Tunisia, Mar. 2017, pp. 1–5.

[13] C. H. Hussaian Basha, S. Rafkiran, E. Touti, B. B. Graba, and M. Aoudia, "A universal source DC-DC boost converter for PEMFC-fed EV systems with optimization-based MPPT controller," Int. Trans. Electr. Energy Syst., vol. 2024, p. 5520331, 2024, doi: 10.1155/2024/5520331.

[14] F. Z. Amatoul and M. Er-raki, "Modeling and simulation of electrical generation systems based on PEM fuel cell-boost converter using a closed loop PI controller," Energy Rep., 2023, doi: 10.1016/j.egyr.2023.08.055.

Power System Technology
ISSN:1000-3673
Received: 06-01-2026 Revised: 15-02-2026 Accepted: 12-03-2026

[15] U. Sarma and S. Ganguly, "Modelling of the PEM fuel cell and design of a closed loop control based DC-DC boost converter for locomotive application," in Proc. IEEE Milan PowerTech, Milan, Italy, Jun. 2019, pp. 1–6, doi: 10.1109/PTC.2019.8810709.

[16] Y. B. Yakut, "A new control algorithm for increasing efficiency of PEM fuel cells—based boost converter using PI controller with PSO method," Int. J. Hydrogen Energy, vol. 75, pp. 1–11, Jul. 2024, doi: 10.1016/j.ijhydene.2023.12.008.

[17] J. Gao, Y. Yang, and H. Gu, "Improving the output power of PEM fuel cell with PI + ASM combined controller designed for boost converter," J. New Mater. Electrochem. Syst., vol. 24, no. 4, pp. 261–269, Oct. 2021.

[18] S. Pattanaik, K. C. Bhuyan, and S. Samal, "Performance analysis of a fuel cell connected to a DC-DC boost converter," Int. J. Renewable Energy Res., vol. 14, no. 4, Dec. 2024.

[19] A. M. Agwa, T. I. Alanazi, H. Kraiem, E. Touti, A. Alanazi, and D. K. Alanazi, "MPPT of PEM fuel cell using PI-PD controller based on golden jackal optimization algorithm," Biomimetics, vol. 8, no. 5, p. 426, 2023, doi: 10.3390/biomimetics8050426.

[20] M. Derbeli, O. Barambones, M. Y. Silaa, and C. Napole, "Real-time implementation of a new MPPT control method for a DC-DC boost converter used in a PEM fuel cell power system," Actuators, vol. 9, no. 4, p. 105, 2020, doi: 10.3390/act9040105.

[21] M. Derbeli, A. Charaabi, O. Barambones, and C. Napole, "High-performance tracking for proton exchange membrane fuel cell system PEMFC using model predictive control," Mathematics, vol. 9, no. 11, p. 1158, 2021, doi: 10.3390/math9111158.

[22] C. Ziogou, S. Voutetakis, M. C. Georgiadis, and S. Papadopoulou, "Model predictive control (MPC) strategies for PEM fuel cell systems—A comparative experimental demonstration," Chem. Eng. Res. Des., vol. 131, pp. 656–670, Mar. 2018.

[23] B. Kanouni, A. E. Badoud, S. Mekhilef, A. Elsanabary, M. Bajaj, and I. Zaitsev, "A fuzzy-predictive current control with real-time hardware for PEM fuel cell systems," Sci. Rep., 2024, doi: 10.1038/s41598-024-78030-0.

[24] E. Irmak and N. Güler, "A model predictive control-based hybrid MPPT method for boost converters," Int. J. Electr., vol. 107, pp. 1–16, 2020.